

**ENRICHMENT, SEPARATION, AND RECOVERY OF PHOSPHORUS FROM DEPHOSPHORIZATION SLAG**

A better understanding of phosphorus distribution in slag is necessary to develop an effective way to treat dephosphorization slag formed during steelmaking. Here, previous studies on the enrichment, separation, and recovery of phosphorus from dephosphorization slag are reviewed, along with their influencing factors. The results suggest that a proper heat treatment can promote the selective enrichment and growth of P-rich phases. Further, adding  $P_2O_5$  and  $Fe_2O_3$  facilitates phosphorus enrichment. Also,  $Ca_3(PO_4)_2$  is precipitated from slag containing 18 wt%  $P_2O_5$ . MnO and MgO in the slag barely affect the phosphorus recovery. In contrast, the addition of  $Al_2O_3$  and  $TiO_2$  significantly affects phosphorus enrichment and magnetic separation. A phosphorus recovery rate of more than 70% is achieved with the addition of 10 wt%  $Al_2O_3$  or 10 wt%  $TiO_2$ . New phases ( $Na_2Ca_4(PO_4)_2SiO_4$ ,  $Na_3PO_4$ , and  $Ca_5(PO_4)_3F$ ) tend to be formed on the addition of  $Na_2O$  and  $CaF_2$ , which promote phosphorus enrichment. However, the addition of  $Na_2O$  and  $CaF_2$  results in the incomplete separation of phosphorus and iron, as  $CaF_2$  and  $Na_2O$  improve slag metallization and the magnetism of iron-rich phases.

*Keywords:* phosphorus enrichment, selective enrichment and growth, P-rich phase, magnetic separation

**1. Introduction**

Dephosphorization is a critical step in steelmaking. Dephosphorization slag based on  $CaO-Fe_2O_3-SiO_2$  has high basicity ( $R$ ) and  $Fe_2O_3$  content. However, the recycle/reuse of this slag is greatly limited by the circulation and enrichment of phosphorus, generating possible contamination in the liquid steel. Therefore, a better understanding of the phosphorus distribution and separating P are very important to promote the reutilization and treatment of dephosphorization slag formed during steelmaking.

Previous studies have proposed many methods of dephosphorization, such as gasification, addition of reductants [1], and floating separation [2]. Additionally, phosphorus is reduced and dissolved in liquid iron to decrease its content in slag [3]. However, few studies have focused on the effective recovery of phosphorus. Furthermore, the phosphorus content in slag is low (4-7%) and dispersed, making it difficult to recover phosphorus for other applications, such as the production of phosphate fertilizers [4]. Therefore, it is necessary to promote the enrichment, growth, and effective recovery of phosphorus from dephosphorization slag. Sui [5-6] has proposed the selective enrichment and separation of phosphorus based on the extraction of valuable components. According to this mechanism, by selectively gathering the dispersed components in the target phase, the efficiency of separating valuable components increases. Similarly, phosphorus is selectively gathered in the P-rich phase. This process improves the enrichment rate and separation efficiency

of phosphorus. Most recent studies [7-12] have focused on the effect of slag basicity, slag composition ( $MgO$ ,  $MnO$ ,  $P_2O_5$ ,  $Fe_2O_3$ ), and additives ( $Na_2O$ ,  $CaF_2$ ,  $Al_2O_3$ ,  $TiO_2$ ) on the selective enrichment, growth, and separation of phosphorus along with the mechanism of phosphorus enrichment [18-21]. However, most of the above studies have focused on laboratory investigations. Therefore, research on the resource utilization of P in industrial production is scarce.

To effectively recycle Fe and P of dephosphorization slag, the effects of slag basicity, slag composition, and additives on the enrichment, separation, and recovery of phosphorus are reviewed. Besides, the challenges and factors associated with “phosphorus enrichment and growth – separation – recycling” have been considered.

**2. Properties of dephosphorization slag****2.1. Phase structure of dephosphorization slag**

$CaO-Fe_2O_3-SiO_2$  slag consists of a P-rich phase, matrix phase, and RO phase [18,19]. As shown in Fig. 1, the P-rich phase in the slag is mainly in the form of a  $nCa_2SiO_4 \cdot Ca_3(PO_4)_2$  solid solution ( $nC_2S-C_3P$ ) and the  $P_2O_5$  content in this solid solution is more than 20% [20,21]. The white RO phase is mainly composed of iron oxides or Fe-Mn oxides. Extra phosphorus is present in the matrix phase.

\* UNIVERSITY OF SCIENCE AND TECHNOLOGY BEIJING, STATE KEY LABORATORY OF ADVANCED METALLURGY BEIJING 100083, CHINA

<sup>#</sup> Corresponding author: gaoming0309@163.com

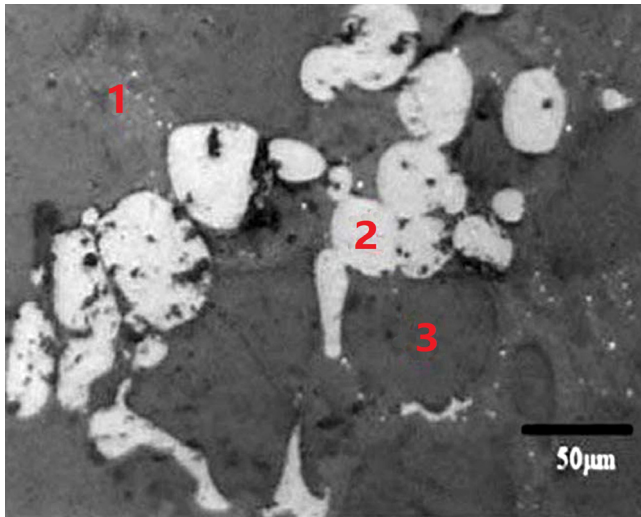


Fig. 1. Main phases in slag (1: matrix phase, 2: RO phase, 3: P-rich phase) [19]

## 2.2. Factors influencing phase structure

### 2.2.1. Slag Basicity

Slag basicity mainly affects the formation of  $x\text{CaO}\cdot\text{SiO}_2$  phase. Then the following phenomenon will happen. Firstly, the  $\text{C}_3\text{S}$  phase is formed in high-basicity slag [8]. Meanwhile, the  $\text{C}_3\text{S}$  reacts with  $\text{P}_2\text{O}_5$  and  $\text{CaO}$  in slag to form  $n\text{C}_3\text{S}\text{-C}_3\text{P}$ . With

decreasing slag basicity, the  $\text{C}_3\text{S}$  content decreases and the  $\text{C}_2\text{S}$  phase is formed. Similarly, solid  $\text{C}_2\text{S}$  particles dissolve in the slag, and the  $n\text{C}_2\text{S}\text{-C}_3\text{P}$  phase is generated. Subsequently, the  $\text{C}_2\text{S}$  phase disappears in low-basicity slag, and a new CS phase is generated, which leads to a decrease in the  $n\text{C}_2\text{S}\text{-C}_3\text{P}$  content. The  $\text{P}_2\text{O}_5$  content in the phases gradually increases in the order of  $n\text{C}_3\text{S}\text{-C}_3\text{P} < n\text{C}_2\text{S}\text{-C}_3\text{P} < \text{C}_3\text{P}$  [8,36].

Lin [8] has analyzed the influence of  $\text{SiO}_2$  modification on phosphorus enrichment in P-bearing steelmaking slag ( $\text{P}_2\text{O}_5 = 10 \text{ wt}\%$ ). According to Fig. 2a,  $\text{C}_3\text{S}$  appears at  $R = 4$  and disappears when  $R = 1\text{-}3$ . Then,  $\text{C}_2\text{S}$  and  $n\text{C}_2\text{S}\text{-C}_3\text{P}$  are formed at 1623 K ( $R = 2.5$ ) as shown in Fig. 2b-d. Finally, CS is formed when  $R < 1.5$ . Son [36] has also reported that  $n\text{C}_2\text{S}\text{-C}_3\text{P}$  is generated in  $\text{CaO}\text{-Fe}_t\text{O}\text{-SiO}_2\text{-}5 \text{ wt}\% \text{ P}_2\text{O}_5$  slag ( $\text{Fe}_t\text{O} = 15\text{-}20 \text{ wt}\%$ ) at  $R = 1$  and  $R = 1.5$ . Therefore, the optimal basicity for generating  $n\text{C}_2\text{S}\text{-C}_3\text{P}$  is 1.5-2.5. Under favorable dynamics conditions, more  $\text{P}_2\text{O}_5$  accumulates near  $\text{C}_2\text{S}$  particles at higher temperatures [31]. Therefore, the phosphorus content in the P-rich phase at 1400°C is higher than that at 1350°C [15].

### 2.2.2 Slag Composition

Previous studies have reported that  $\text{MnO}$  and  $\text{MgO}$  mainly enter into the RO phase to form  $\text{MgFe}_2\text{O}_4$  and  $\text{MnFe}_2\text{O}_4$ , and different  $\text{P}_2\text{O}_5$  and  $\text{Fe}_t\text{O}$  contents affect the form of the  $\text{C}_x\text{S}$  phase [9-11,36].

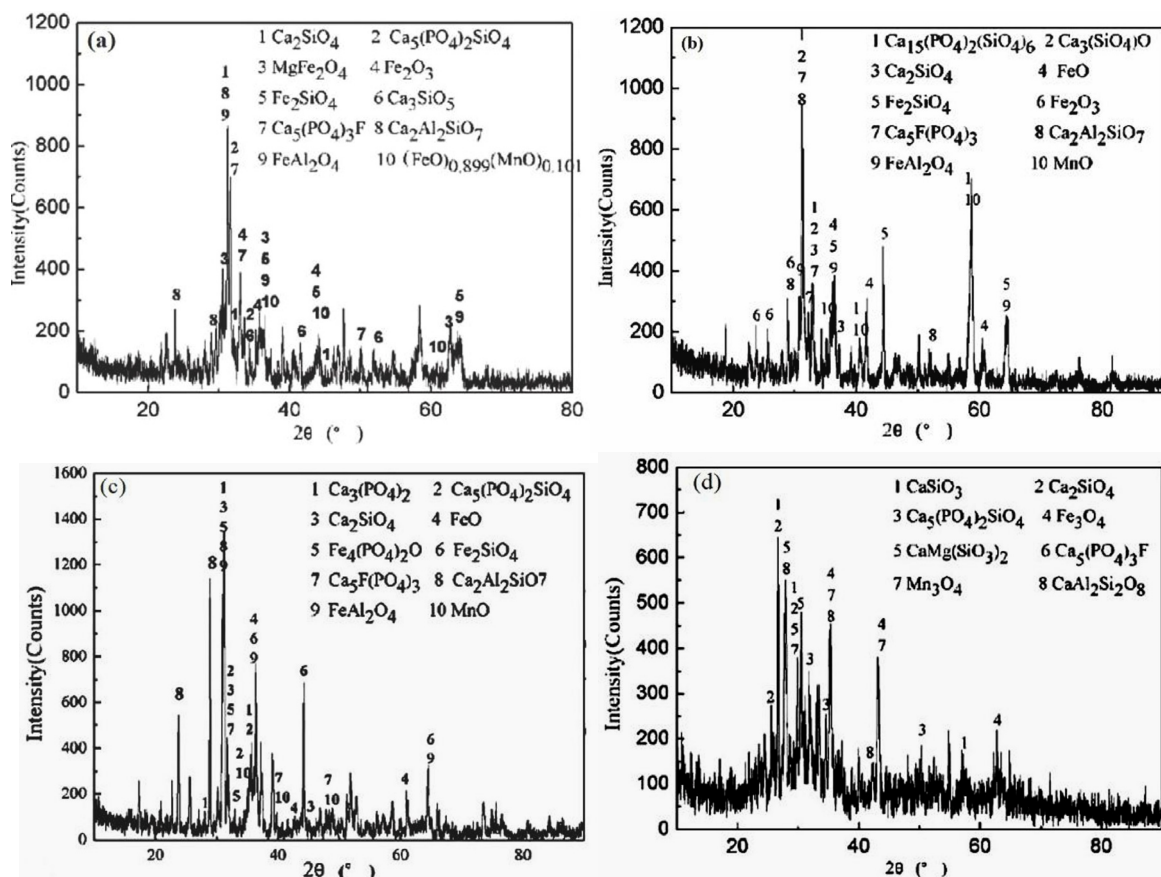


Fig. 2. X-ray diffraction patterns (a:  $R = 4$ , b:  $R = 3$ , c:  $R = 2$ , d:  $R = 1$ ) [8]

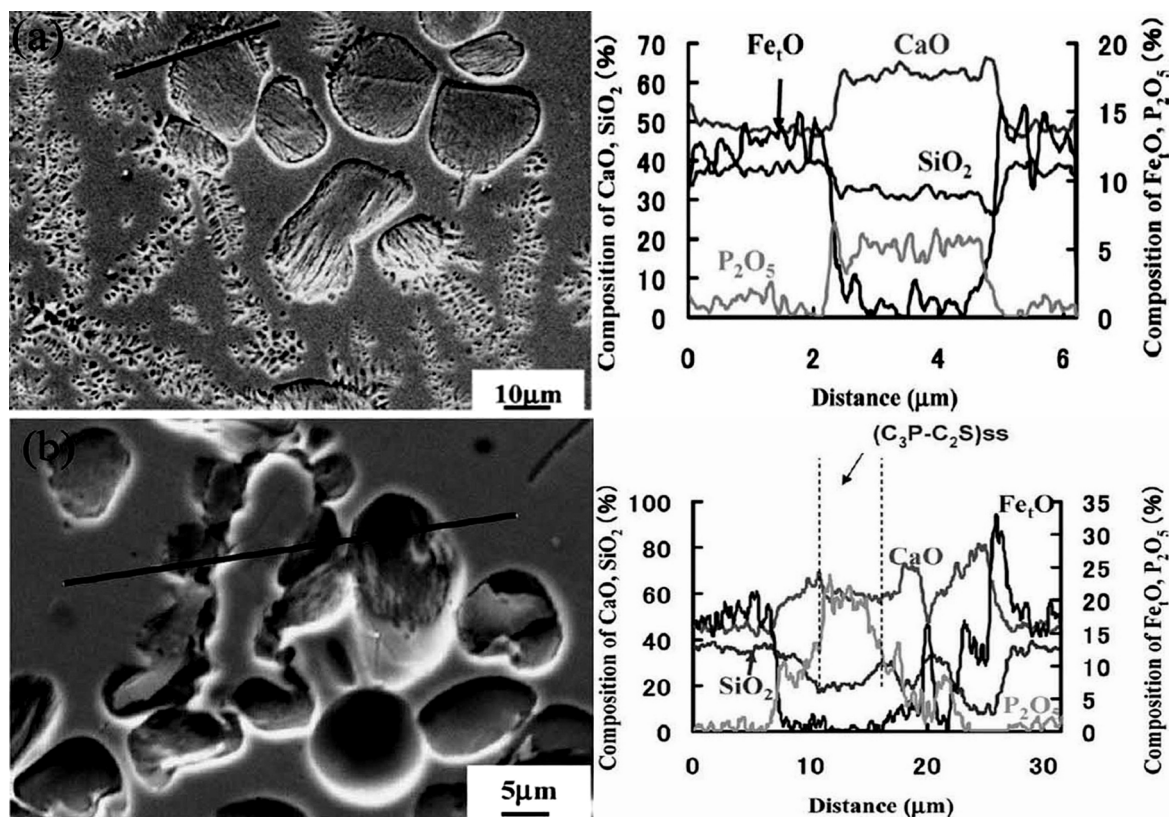


Fig. 3. Results of SEM and line scanning (a: 10 wt% Fe<sub>t</sub>O, b: 15 wt% Fe<sub>t</sub>O) [36]

Son [36] has reported the effect of elemental compositions on CaO-Fe<sub>t</sub>O-SiO<sub>2</sub>-5 wt% P<sub>2</sub>O<sub>5</sub> slag (CaO/SiO<sub>2</sub> = 1.5). Fig. 3a shows that CS and C<sub>2</sub>S are generated at Fe<sub>t</sub>O = 10 wt%. However, according to Fig. 3b, C<sub>3</sub>P and *n*C<sub>2</sub>S-C<sub>3</sub>P are formed when the Fe<sub>t</sub>O content is high (Fe<sub>t</sub>O = 15-20 wt%).

Compared with Fe<sub>t</sub>O, the initial P<sub>2</sub>O<sub>5</sub> content in the slag changes the form of the P-rich phase [7,9-11]. Li [7] has examined the behavior of phosphorus enrichment in CaO-FeO-Fe<sub>2</sub>O<sub>3</sub>-SiO<sub>2</sub>-P<sub>2</sub>O<sub>5</sub> slag and has found that the initial P<sub>2</sub>O<sub>5</sub> content promotes the generation of *n*C<sub>2</sub>S-C<sub>3</sub>P. Meanwhile, C<sub>3</sub>P is formed

when more than 18 wt% P<sub>2</sub>O<sub>5</sub> is added [9-11]. The results in Fig. 4 show that CaO<sub>15</sub>(P<sub>2</sub>O<sub>5</sub>)<sub>2</sub>(SiO<sub>2</sub>)<sub>6</sub> is generated with the addition of less than 18 wt% P<sub>2</sub>O<sub>5</sub>, and C<sub>3</sub>P is formed when the P<sub>2</sub>O<sub>5</sub> content is up to 18 wt%. C<sub>3</sub>P has lower Gibbs free energy than C<sub>2</sub>S; therefore, it is more stable in the temperature range 400-1800°C. Further, compared to SiO<sub>2</sub>, P<sub>2</sub>O<sub>5</sub> can more easily combine with CaO. Hence, CaO preferentially combines with P<sub>2</sub>O<sub>5</sub> and C<sub>3</sub>P is formed [9].

In summary, MgO and MnO have little effect on the P-rich phase. Appropriate P<sub>2</sub>O<sub>5</sub> and Fe<sub>t</sub>O contents promote the precipitation of the P-rich phase. *n*C<sub>2</sub>S-C<sub>3</sub>P and C<sub>3</sub>P are formed with the addition of more than 15 wt% Fe<sub>t</sub>O and 18 wt% P<sub>2</sub>O<sub>5</sub>, respectively.

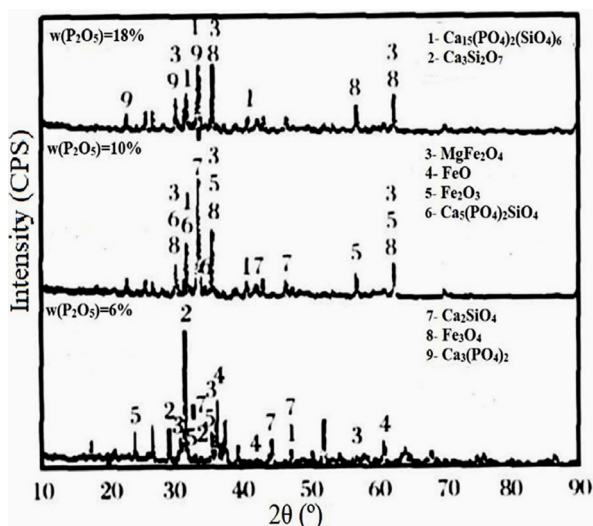
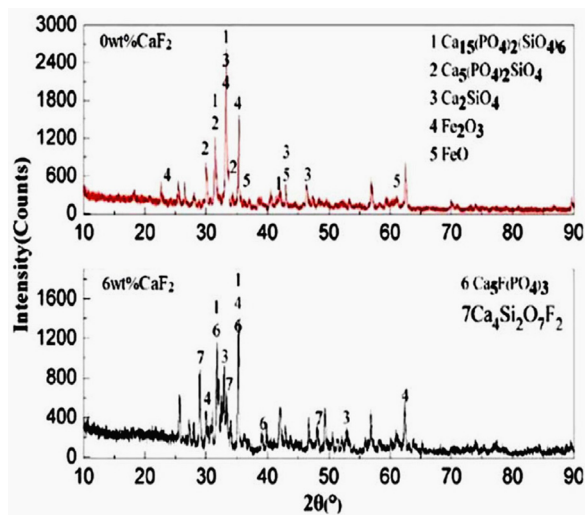
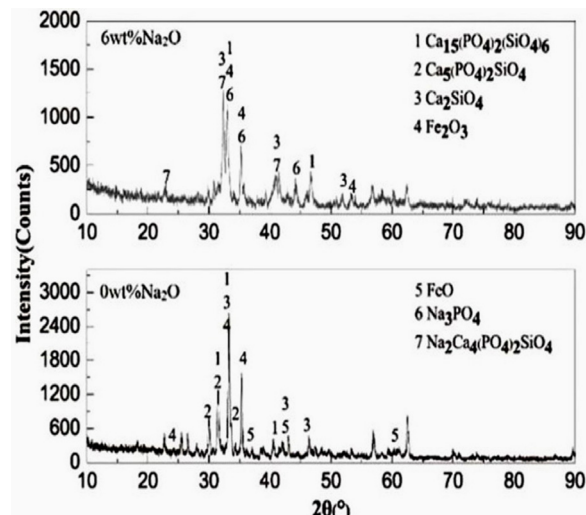


Fig. 4. Effect of P<sub>2</sub>O<sub>5</sub> content on precipitated phase [9]

### 2.2.3. Addition of CaF<sub>2</sub> and Na<sub>2</sub>O

Many studies have shown that adding CaF<sub>2</sub> and Na<sub>2</sub>O changes the primary phase and phosphorus form, respectively [40,41]. Fig. 5 shows that 6C<sub>2</sub>S-C<sub>3</sub>P and C<sub>2</sub>S-C<sub>3</sub>P are generated in fluorine-free modified slag. A new phase, Ca<sub>5</sub>(PO<sub>4</sub>)<sub>3</sub>F, is generated on the addition of 6 wt% CaF<sub>2</sub>. Therefore, the *n*C<sub>2</sub>S-C<sub>3</sub>P and Ca<sub>5</sub>(PO<sub>4</sub>)<sub>3</sub>F phases are mainly considered to be P-rich phases [40]. Fig. 6 shows that Na<sub>2</sub>O-free modified slag consists of 6C<sub>2</sub>S-C<sub>3</sub>P, C<sub>2</sub>S-C<sub>3</sub>P, C<sub>2</sub>S, and RO phases. However, Na<sub>2</sub>Ca<sub>4</sub>(PO<sub>4</sub>)<sub>2</sub>SiO<sub>4</sub> is formed in Na<sub>2</sub>O-bearing slag. Meanwhile, Na<sub>3</sub>PO<sub>4</sub> is generated in slag containing 6 wt% Na<sub>2</sub>O [41].

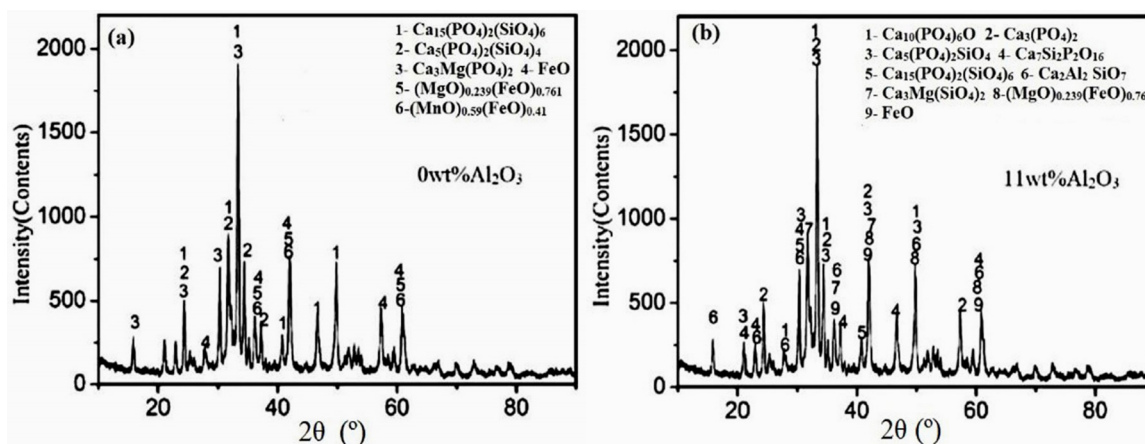
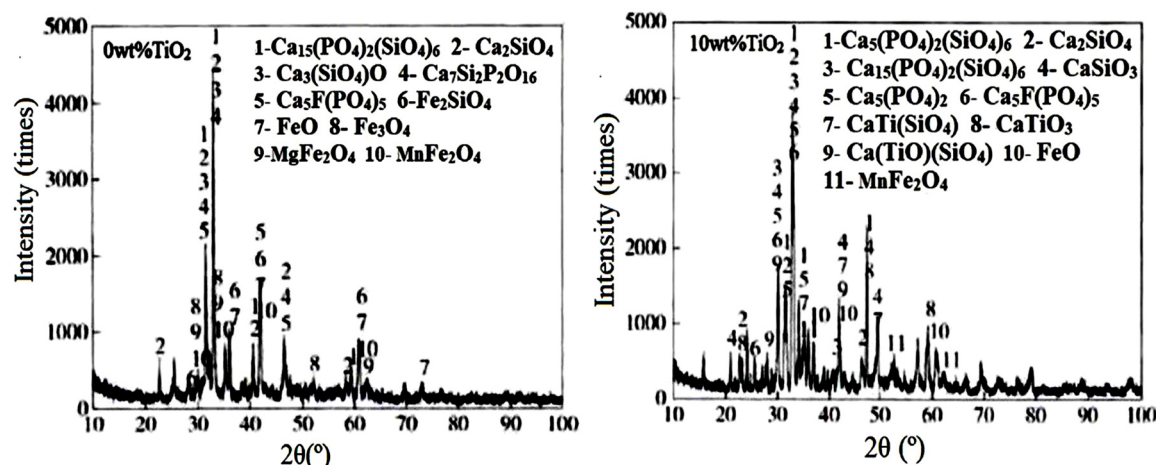
Fig. 5. CaF<sub>2</sub>-modified slag [40]Fig. 6. Na<sub>2</sub>O-modified slag [41]

### 2.2.4. Addition of Al<sub>2</sub>O<sub>3</sub> and TiO<sub>2</sub>

Most studies have revealed that Al<sub>2</sub>O<sub>3</sub> and TiO<sub>2</sub> modification are beneficial to increase the phosphorus content in the P-rich phase [42-45]. Jiang [43] has examined the effect of Al<sub>2</sub>O<sub>3</sub> on the phosphorus form existing in CaO-SiO<sub>2</sub>-10 wt% FeO-6

wt% MgO-4 wt% MnO-10 wt% P<sub>2</sub>O<sub>5</sub>-Al<sub>2</sub>O<sub>3</sub> slag. According to Fig. 7b, Ca<sub>2</sub>Al<sub>2</sub>SiO<sub>7</sub> is generated in Al<sub>2</sub>O<sub>3</sub>-bearing slag, along with the matrix, RO, and P-rich phases. Further, C<sub>3</sub>P is formed on adding 11 wt% Al<sub>2</sub>O<sub>3</sub>.

Lin [45] has reported the effect of TiO<sub>2</sub> modification on phosphorus enrichment in industrial slag by adding 10 wt%

Fig. 7. X-ray diffraction patterns of Al<sub>2</sub>O<sub>3</sub>-modified slag [43]Fig. 8. X-ray diffraction patterns of TiO<sub>2</sub>-modified slag [45]

$P_2O_5$ . As shown in Fig. 8a,  $TiO_2$ -free modified slag consists of the matrix, RO, and  $CaO_{15}(P_2O_5)_2(SiO_2)_6$  phases. However, new phases ( $CaTiO_3$ ,  $CaSiTiO_4$ ) are generated after adding 10 wt%  $TiO_2$  (Fig. 8b).  $[TiO_6]$ , an important part of  $MgFe_2O_4$ - $Mg_2TiO_4$  and  $CaTiO_3$ , is formed after adding  $TiO_2$ . Furthermore,  $[TiO_4]$  and  $[SiO_4]$  can be copolymerized to form  $CaSiTiO_4$ , and  $C_2S$  in  $nC_2S$ - $C_3P$  is robbed  $CaSiTiO_4$  to generate  $yC_2S$ - $C_3P$  ( $y < n$ ) [4]. Therefore, new phases are generated on adding  $Al_2O_3$  and  $TiO_2$ .

### 2.2.5. Temperature and cooling conditions

Su [33] has reported the distribution of phase structure in  $CaO$ - $SiO_2$ - $Fe_2O_3$ - $P_2O_5$  slag under  $1350^\circ C$  and  $1400^\circ C$ . After holding 600s, the slag consists of  $C_2S$ - $C_3P$  phase and matrix phase. However, Fig. 9 shows that  $C_2S$ - $C_3P$  phase is blocked under  $1350^\circ C$ . Therefore, the lower temperature promotes the enrichment of  $P_2O_5$ .

In addition, the cooling conditions have effect on phase structure. Li [18] has reported the P-rich phase in steel slag under water quench process and hot splash process. The P-rich phase under water quench process is  $nC_2S$ - $C_3P$ , while it is  $C_3P$  under hot splash process. Wu [23] has reported the distribution in  $SiO_2$  modified slag. The results show that P is gathered to  $C_2S$  phase when the cooling rates are  $1^\circ C \cdot min^{-1}$  and  $3^\circ C \cdot mmin^{-1}$ . The  $C_2S$  phase are spherical and arborization. However, the  $C_2S$  phase is arborization and punctate when the cooling rate is  $5^\circ C \cdot min^{-1}$ .

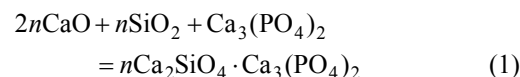
## 3. Phosphorus enrichment in dephosphorization slag

### 3.1 Mechanism of phosphorus enrichment

The mechanism of phosphorus enrichment can be concluded from the following process. First, solid  $C_2S$  particles dissolve in the slag. Then  $nC_2S$ - $C_3P$  is generated in the multi-phase area where solid and liquid phases coexist. Finally, the solid-solution

layer is extended and completely changes into the  $nC_2S$ - $C_3P$  layer with the shrinking of the solid  $C_2S$  particles [21-27].

According to the slag ionic structure theory [22], slag consists of oxides, compounds, and charged protons (ions). As the  $SiO_2$  content in basic dephosphorization slag is higher than the  $P_2O_5$  and  $Al_2O_3$  contents,  $C_2S$  and  $C_3S$  based on  $SiO_4^{4-}$  are generated during solidification, and  $SiO_4^{4-}$  is more easily replaced by  $P_2O_5$  and  $Al_2O_3$ . Then, phosphorus is precipitated as  $PO_4^{3-}$  and coexists with  $SiO_4^{4-}$ . Therefore, it is difficult to generate  $C_3P$  in dephosphorization slag. The formation reaction of  $nC_2S$ - $C_3P$  can be expressed as Eq. (1).



It is well known that  $C_3S$  and  $C_2S$  react with  $C_3P$  to form a solid solution. Hence, the phosphorus in the slag is distributed in multiple phases [23]. Stable  $C_3S$  changes to spherical  $C_2S$  at  $1300^\circ C$ . Therefore, the P-rich phase mainly occurs in the  $nC_2S$ - $C_3P$  phase as  $C_3S$  cannot react with  $C_3P$  at any ratio.

Most researchers have reported the behavior of mass transfer between single  $C_2S$  particles and slag [24-27].  $C_2S$  particles are regarded as a multi-layered filter paper. Here the phosphorus in the slag is filtered and the phosphorus content gradually decreases in the direction of the  $C_2S$  particles. Therefore,  $nC_2S$ - $C_3P$  is generated until the  $C_2S$  particles disappear. Fig. 10 shows the reaction between  $C_2S$  particles and  $CaO$ - $SiO_2$ - $Fe_2O_3$ - $P_2O_5$  slag at  $1500^\circ C$  for 300 s. It reveals that a solid-solution layer is formed between the slag and the  $C_2S$  particles after 1 s (Fig. 10a), and after 60 s (Fig. 10b-c), the number of  $C_2S$  particles decrease with increasing area of this solid-solution layer [27]. Ono [24] has reported that ferrous and iron oxides increase the activity coefficient of  $C_3P$  in  $CaO$ - $SiO_2$ - $FeO$ / $Fe_2O_3$  slag. Most of the  $P_2O_5$  in the slag reacts with  $C_2S$  particles to generate a solid solution. Moreover, the products float to the top of the slag. Ito [25] has measured the distribution ratio between  $CaO$ - $SiO_2$ - $FeO$ / $Fe_2O_3$  slag and  $C_2S$  particles. The results reveal that 80%  $P_2O_5$  is transferred from the slag to the surface of the  $C_2S$  particles to form  $nC_2S$ - $C_3P$ . Wang [26] has analyzed the enrichment be-

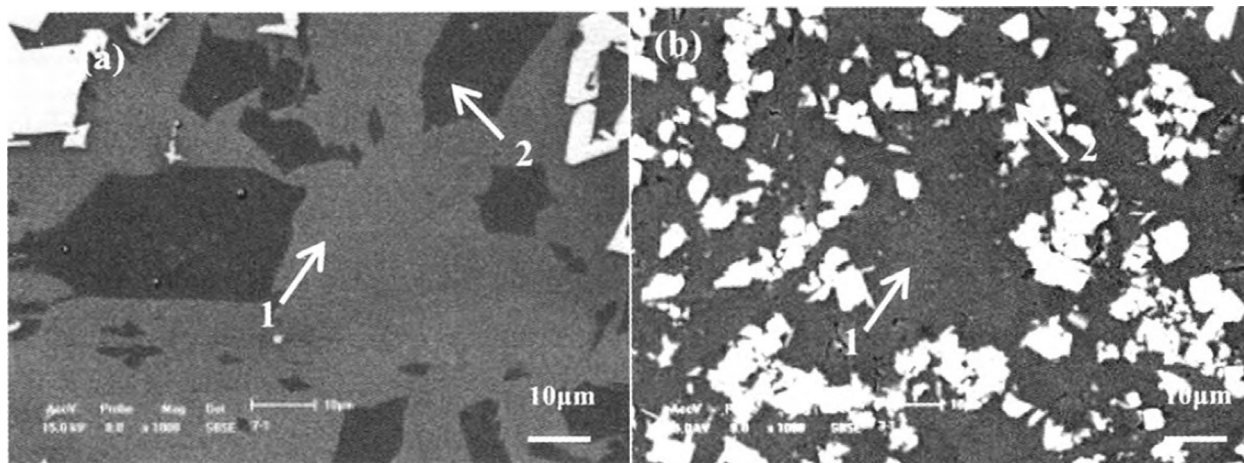


Fig. 9. The phase structure at different temperatures:(a)  $1350^\circ C$  and (b)  $1400^\circ C$  (1: matrix phase, 2: P-rich phase) [33]

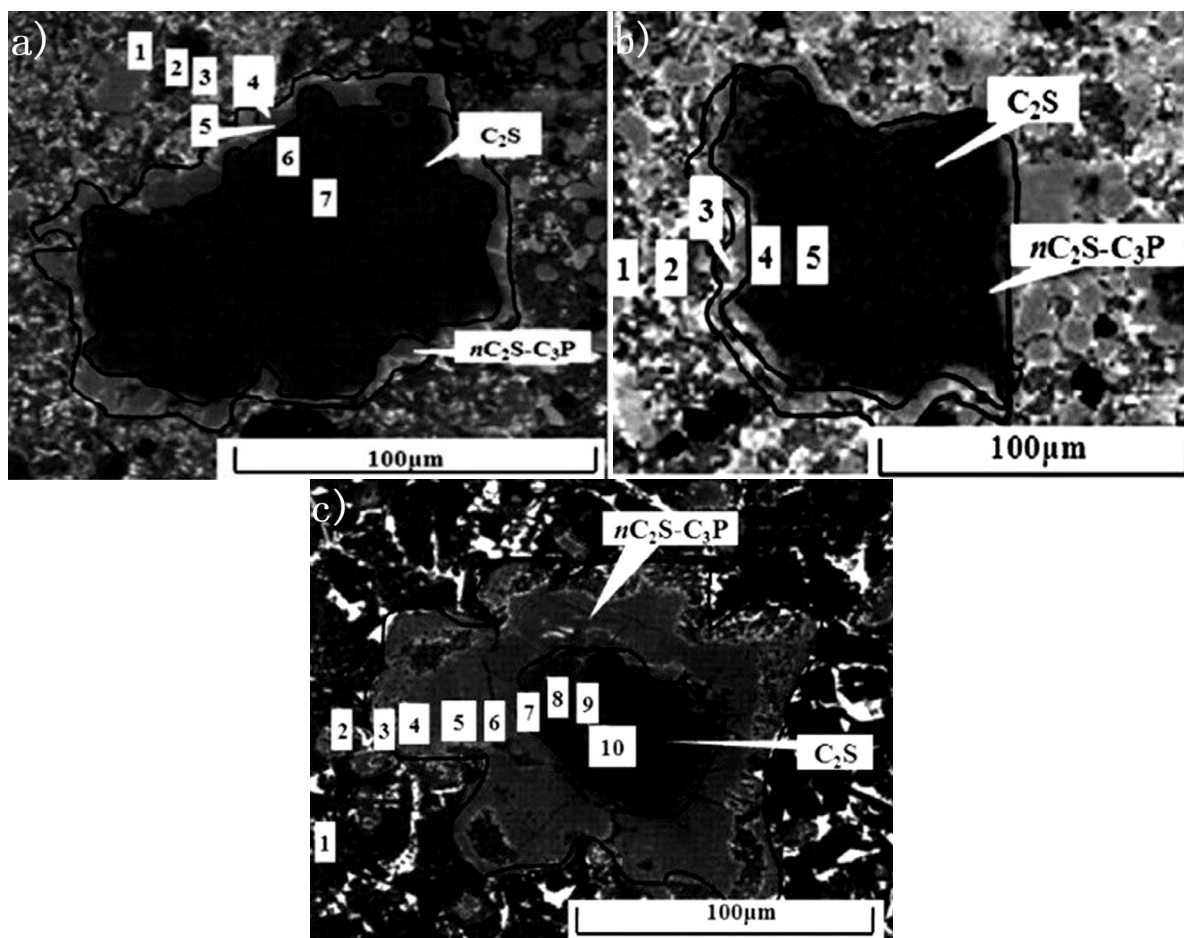


Fig. 10. SEM results at different times: (a)1s, (b)60s, and (c)300s [27]

havior of  $\text{CaO-SiO}_2\text{-Fe}_t\text{O-P}_2\text{O}_5$  slag at  $1400^\circ\text{C}$  and has found that  $\text{C}_2\text{S}$  particles provide space for phosphorus enrichment. Therefore, phosphorus diffuses from the slag to the surface of the  $\text{C}_2\text{S}$  particles.

Furthermore, a macro-process for phosphorus enrichment has been proposed. Yang et. al [28-30] have reported the reaction between  $\text{C}_2\text{S}$  particles and  $\text{CaO-SiO}_2\text{-FeO}_x\text{-P}_2\text{O}_5$  slag at  $1400^\circ\text{C}$  for 60 s. The mechanism is illustrated in Fig. 11.

- 1)  $\text{C}_2\text{S}$  particles dissolve into the slag and the slag penetrates into the solid sample (Fig. 11a).
- 2) The edge of the solid  $\text{C}_2\text{S}$  particles changes into a multi-phase area where solid and liquid phases coexist (Fig. 11b).
- 3) In this multi-phase area,  $\text{CaO}$  and  $\text{P}_2\text{O}_5$  react with the  $\text{C}_2\text{S}$  particles to form  $n\text{C}_2\text{S-C}_3\text{P}$  (Fig. 11c).
- 4) The multi-phase area shifts toward the side of the  $\text{C}_2\text{S}$  particles to form a new P-rich phase (Fig. 11d).
- 5) The previously formed P-rich phase is either retained (Fig. 11e1), partly dissolved (Fig. 11e2), or fully dissolved into the slag (Fig. 11e3). The P-rich phase region is gradually extended.

Suito [31] has examined the behavior of phosphorus diffusion from  $\text{CaO-Fe}_t\text{O-P}_2\text{O}_5\text{(-SiO}_2\text{)}$  slag to  $\text{CaO}$  particles at  $1400^\circ\text{C}$ . The results show that  $n\text{C}_2\text{S-C}_3\text{P}$  is generated at the surface of  $\text{CaO}$  particles within 30 s. After 5 min,  $\text{CaO-Fe}_t\text{O}$  is produced between the  $n\text{C}_2\text{S-C}_3\text{P}$  and  $\text{CaO}$  particles. Inoue

[32] has reported the phosphorus distribution between  $\text{CaO-Fe}_t\text{O-P}_2\text{O}_5$  slag and  $\text{C}_2\text{S}$  particles. The results show that all the phosphorus in  $\text{C}_2\text{S}$  particles ( $20\text{-}50\ \mu\text{m}$ ) is converted into  $n\text{C}_2\text{S-C}_3\text{P}$  in less than 5 s. Only the rim part of the particles ( $5\ \mu\text{m}$ ) and the small particles ( $3\text{-}8\ \mu\text{m}$ ) change to  $n\text{C}_2\text{S-C}_3\text{P}$  within 5 s when the particles are clustered. However, this phenomenon is not observed in  $\text{CaO-SiO}_2\text{-Fe}_t\text{O-P}_2\text{O}_5$  slag.

Consequently, the formation of the P-rich phase can be described by the following process. The phosphorus in the slag transfers to the  $\text{C}_2\text{S}$  particles at high temperatures and reacts with  $\text{C}_2\text{S}$  to generate  $n\text{C}_2\text{S-C}_3\text{P}$ , and the previously formed P-rich phase is replaced by new products.

## 3.2. Factors influencing selective enrichment

### 3.2.1. Concept of Selective Enrichment

Temperature and the size of the  $\text{C}_2\text{S}$  particles affect phosphorus enrichment [26,33]. Because a higher temperature improves the kinetics of slag formation, the phosphorus content in the P-rich phase at  $1400^\circ\text{C}$  is higher than that at  $1350^\circ\text{C}$  [26,33]. The size of the P-rich phase increases with increasing enrichment time [33], and  $\text{C}_2\text{S}$  particles, of size less than  $50\ \mu\text{m}$ , are completely converted to form a P-rich phase [26].

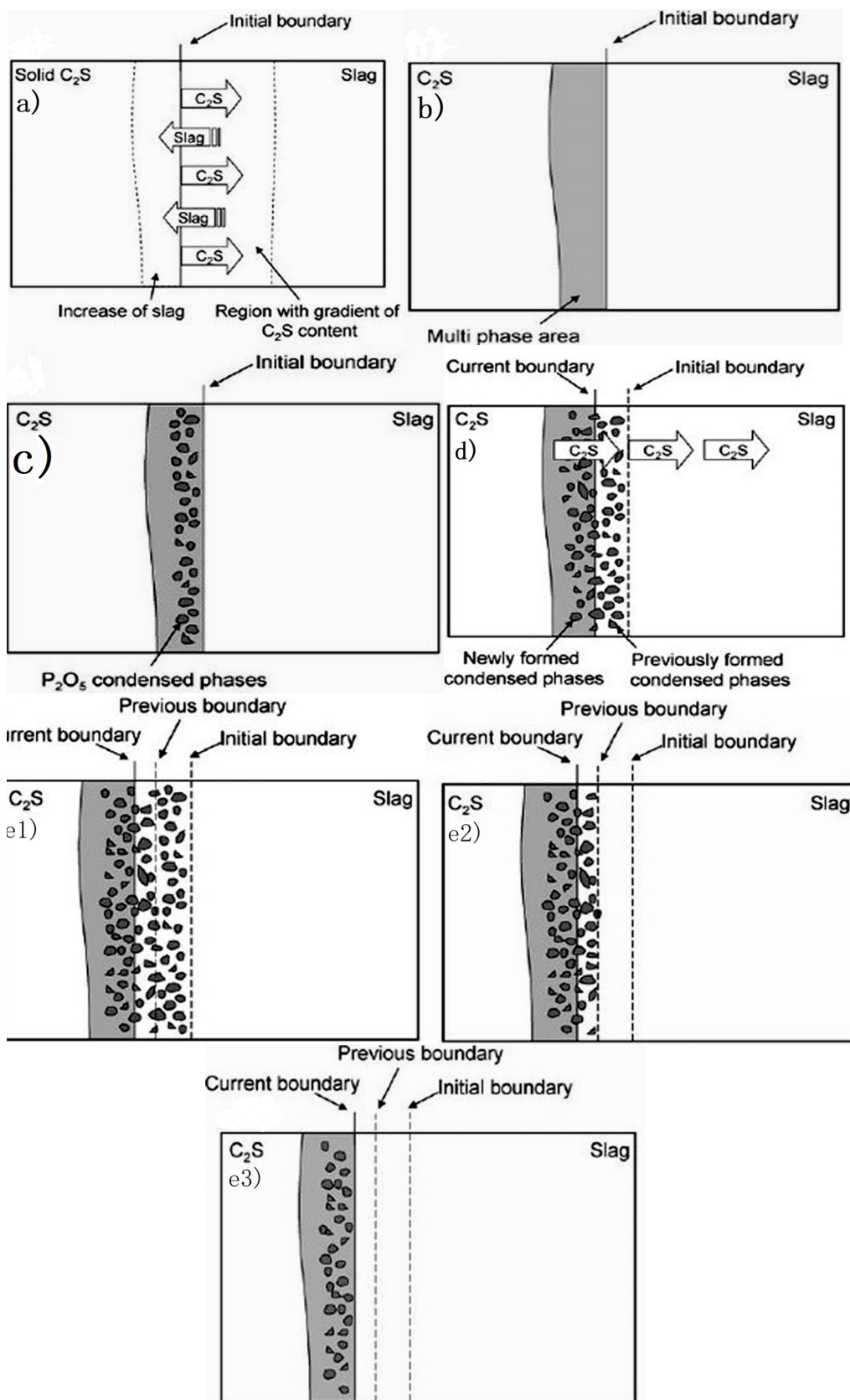


Fig. 11. Formation mechanism of  $nC_2S-C_3P$  [28]

However, the phosphorus content in the P-rich phase is low and dispersed. Therefore, the selective enrichment of P is important to increase the enrichment, separation, and recovery of the P-rich phase [34,35]. In 1978, Jha [34] proposed the concept of

selective precipitation to obtain nickel sulfide and cobalt sulfide. In China, Sui [35] has proposed the technology of selective enrichment and separation. "Selective enrichment" means that suitable thermodynamics and kinetics are achieved by changing

the slag compositions and additives. Then, valuable components interspersed in each phase are selectively transferred. Eventually, the valuable components accumulate in the target phase due to chemical gradient. The slag basicity and composition, the initial content of  $P_2O_5$ , and the value of  $(\%FeO)/(\%CaO)$  have effect on the selective enrichment.

### 3.2.2. Slag Basicity and Composition

Using a suitable slag basicity is a good method to promote selective enrichment. Zhou [11] has examined the behavior of distribution of phosphorus between the P-rich phase and the matrix phase. The results show that phosphate capacities increase with decreasing slag basicity. According to Fig. 12, the  $P_2O_5$  content in the P-rich phase decreases with increasing slag basicity. Lin [8] has reported the influence of  $SiO_2$  modification on the phosphorus enrichment in P-bearing steelmaking slag. The results show that the  $P_2O_5$  contents in the P-rich phase were 19-25 wt%, 31-32 wt%, 32-33 wt%, and 34-37 wt% for  $R$  values decreasing from 4 to 1, respectively. Son [36] has analyzed  $CaO$ -20 wt%  $Fe_tO$ - $SiO_2$ -5 wt%  $P_2O_5$  slag and has found that the  $P_2O_5$  content was 37.3 wt% and 22.7 wt% at  $R = 2.0$  and  $R = 2.5$ , respectively. Thus, a higher slag basicity is harmful to phosphorus enrichment.

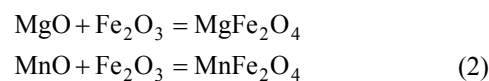
Many studies have reported the effect of slag compositions ( $MgO$ ,  $MnO$ ,  $P_2O_5$ ,  $Fe_tO$ ) on the selective enrichment of the P-rich phase. The addition of  $P_2O_5$  increases the phosphorus content in the P-rich phase, whereas  $MgO$  and  $MnO$  have little effect [9-11,15,36-39].

$Fe_tO$  is an inevitable component in slag and reduces polymerization and viscosity. Additionally, it contributes to mass transfer and phosphorus enrichment in dephosphorization slag [4]. Son [36] has analyzed the effect of  $Fe_tO$  on  $CaO$ - $Fe_tO$ - $SiO_2$ -5 wt%  $P_2O_5$  slag. As shown in Fig. 13, the  $P_2O_5$  content in the P-rich phase is 17.6 wt% and 22.7 wt% with the addition of 10 wt%  $Fe_tO$  and 20 wt%  $Fe_tO$ , respectively. Moreover, the common effect of  $Fe_tO$  and  $CaO$  on slag is unclear [7,37,38]. Li [7] has analyzed the effect of  $Fe_tO/CaO$  content on  $CaO$ - $FeO$ - $Fe_2O_3$ - $SiO_2$ - $P_2O_5$  slag and found that  $nC_2S$ - $C_3P$  decreases with increasing  $Fe_tO/CaO$  content.

Zhou [9] has reported the effect of initial  $P_2O_5$  content on phosphorus enrichment in  $CaO$ - $Fe_tO$ - $SiO_2$ - $P_2O_5$  slag. According to Figure 12, when the  $P_2O_5$  content is increased from 6 wt% to 8 wt%, the phosphorus content in the P-rich phase increases from 20.33 wt% to 33.99 wt% and reaches a maximum value (34.91 wt%) when 18 wt%  $P_2O_5$  is added. This suggests that phosphorus content in the P-rich phase increases with increasing initial  $P_2O_5$  content.

$MgFe_2O_4$  and  $MnFe_2O_4$  generated by  $MgO$ ,  $MnO$ , and  $Fe_2O_3$  enter into the RO phase, as shown in Eq. (2) [11,15,39]. Lin [15] has analyzed the effect of  $MgO$  and  $MnO$  on phosphorus enrichment in  $CaO$ - $SiO_2$ -30wt% $Fe_2O_3$ - $MgO$ - $MnO$ -10wt% $P_2O_5$  slag. According to Figure 12, when the  $MgO$  content increases from 5 wt% to 10 wt%, the  $P_2O_5$  content in the P-rich phase

changes from 20.76 wt% to 19.66 wt%. Similarly, when the  $MnO$  content increases from 5 wt% to 10 wt%, the  $P_2O_5$  changes from 22.62 wt% to 19.66 wt%. Thus,  $P_2O_5$  content in the P-rich phase does not change significantly.



In summary,  $MgO$  and  $MnO$  have little effect on the selective enrichment of the P-rich phase. In contrast, the  $P_2O_5$  content in the P-rich phase reaches 20 wt% and 35 wt% on the addition of 15 wt%  $Fe_tO$  and 18 wt%  $P_2O_5$ , respectively.

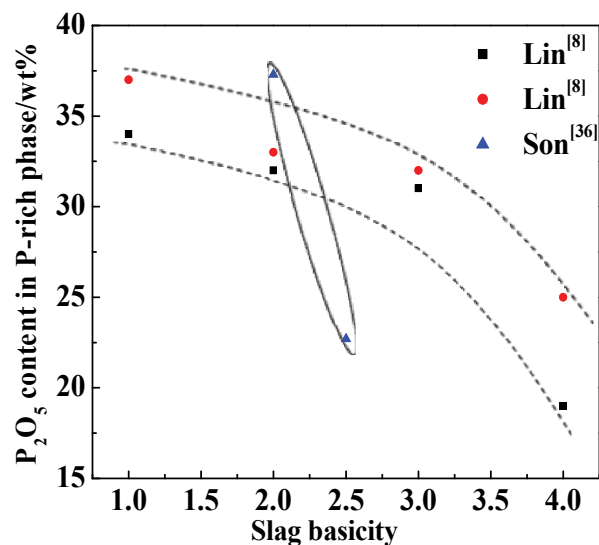


Fig. 12. Effect of slag basicity on  $P_2O_5$  content

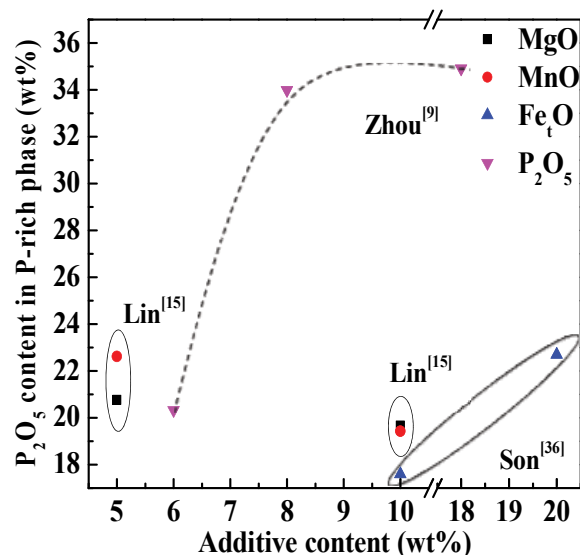


Fig. 13. Effect of slag composition on  $P_2O_5$  content

### 3.2.3. Addition of $CaF_2$ and $Na_2O$

$CaF_2$  and  $Na_2O$  can significantly reduce the melting point of slag and promote phosphorus enrichment [4,11,40,41]. Wang [4] has analyzed the effect of  $CaF_2$  on crystallization in  $CaO$ -



SiO<sub>2</sub>-Fe<sub>1</sub>O-MgO-P<sub>2</sub>O<sub>5</sub>-CaF<sub>2</sub> slag. The results show that the P<sub>2</sub>O<sub>5</sub> content in Ca<sub>5</sub>(PO<sub>4</sub>)<sub>3</sub>F reduces to 28.35 wt% with the addition of 3 wt% CaF<sub>2</sub>. According to Fig. 14, on adding 3 wt% CaF<sub>2</sub> into the slag, the P<sub>2</sub>O<sub>5</sub> content in the P-rich phase is 32.5 wt%, and on adding 6 wt% CaF<sub>2</sub> into the slag, the P<sub>2</sub>O<sub>5</sub> content in the P-rich phase increases to 35.65 wt% [11]. Meanwhile, Lin [40] has reported the phosphorus enrichment behavior in CaO-SiO<sub>2</sub>-Fe<sub>1</sub>O-MgO-P<sub>2</sub>O<sub>5</sub>-CaF<sub>2</sub> slag. The results reveal that the P<sub>2</sub>O<sub>5</sub> content in the P-rich phase is 20.75 wt% in fluorine-free modified slag. On increasing the CaF<sub>2</sub> content from 3 wt% to 6 wt%, the P<sub>2</sub>O<sub>5</sub> content in the P-rich phase increases from 34.0 wt% to 37.75 wt%. Furthermore, it is necessary to control the CaF<sub>2</sub> content to avoid lining erosion and environmental pollution.

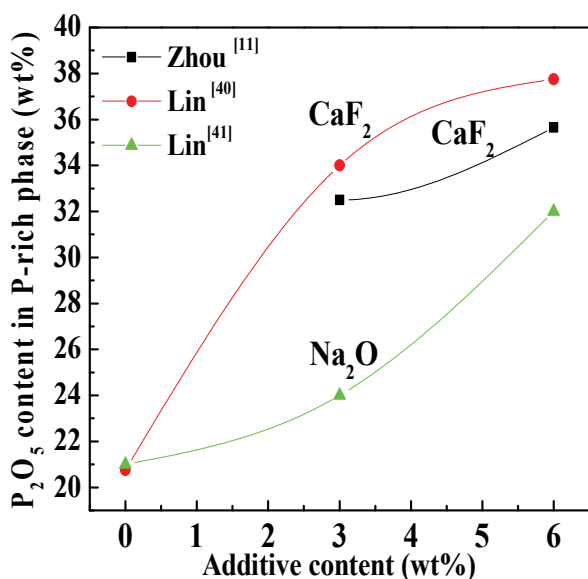
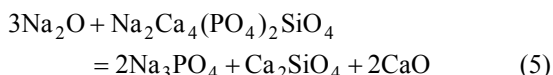
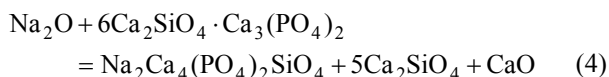
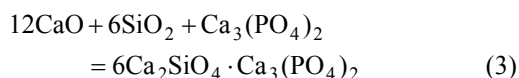


Fig. 14. Effect of addition of CaF<sub>2</sub> and Na<sub>2</sub>O on selective enrichment of phosphorus

The form of phosphorus in the P-rich phase changes on the addition of Na<sub>2</sub>O according to Eqs. (3-5) [41].



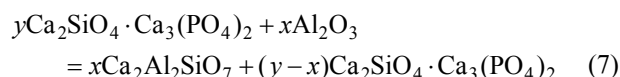
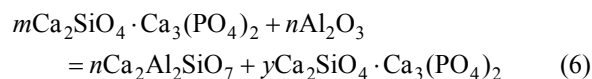
As shown in Eq. (3), 6C<sub>2</sub>S-C<sub>3</sub>P is precipitated in the previous stage of cooling. Then Na<sub>2</sub>Ca<sub>4</sub>(PO<sub>4</sub>)<sub>2</sub>SiO<sub>4</sub> is generated by the reaction of 6C<sub>2</sub>S-C<sub>3</sub>P and Na<sub>2</sub>O at 1623 K (Eq. (4)). Moreover, Na<sub>3</sub>PO<sub>4</sub> is formed in the presence of excess Na<sub>2</sub>O content (Eq. (5)). Lin [41] has reported the influence of Na<sub>2</sub>O on phosphorus enrichment in CaO-SiO<sub>2</sub>-Fe<sub>1</sub>O-MgO-P<sub>2</sub>O<sub>5</sub> slag. As shown in Fig. 14, the P<sub>2</sub>O<sub>5</sub> content in the P-rich phase is 21 wt% in Na<sub>2</sub>O-free modified slag. When the Na<sub>2</sub>O content is increased from 3 wt% to 6 wt%, the P<sub>2</sub>O<sub>5</sub> content in the P-rich

phase increases from 24 wt% to 32 wt%. According to the slag ionic structure theory, the combination of Na<sup>+</sup> and phosphorus ions is stronger than that of Ca<sup>2+</sup> and phosphorus ions. Moreover, Ca<sup>2+</sup> in 6C<sub>2</sub>S-C<sub>3</sub>P or Na<sub>2</sub>Ca<sub>4</sub>(PO<sub>4</sub>)<sub>2</sub>SiO<sub>4</sub> is replaced by Na<sup>+</sup>. Further, Na<sub>3</sub>PO<sub>4</sub> is generated when sufficient Na<sub>2</sub>O is added.

Thus, the P<sub>2</sub>O<sub>5</sub> content in the P-rich phase increases to 30 wt% on adding 3 wt% CaF<sub>2</sub> or 6 wt% Na<sub>2</sub>O. Furthermore, considering the limitations of CaF<sub>2</sub>, it can be replaced by Na<sub>2</sub>O to promote the selective enrichment of phosphorus.

### 3.2.4. Addition of Al<sub>2</sub>O<sub>3</sub> and TiO<sub>2</sub>

Previous studies have shown that Al<sub>2</sub>O<sub>3</sub> and TiO<sub>2</sub> modification are beneficial to phosphorus enrichment [42-45]. The mechanism of Al<sub>2</sub>O<sub>3</sub> modification can be illustrated as shown in Eqs. (6-7) [42-44].



First, *m*C<sub>2</sub>S-C<sub>3</sub>P is precipitated at 1623 K and gradually decreases with the generation of *y*C<sub>2</sub>S-C<sub>3</sub>P (*y* < *n*) (Eq. (6)). Then (*y* - *x*)C<sub>2</sub>S-C<sub>3</sub>P is produced on adding Al<sub>2</sub>O<sub>3</sub> (Eq. (7)). Finally, C<sub>2</sub>S in *y*C<sub>2</sub>S-C<sub>3</sub>P disappears when the Al<sub>2</sub>O<sub>3</sub> content is sufficient to make *y* = *x*, and C<sub>3</sub>P is precipitated from the slag.

As shown in Fig. 15, Diao [44] has revealed that the P<sub>2</sub>O<sub>5</sub> content in the P-rich phase reached 5.1 wt% on adding 8 wt% Al<sub>2</sub>O<sub>3</sub> into CaO-SiO<sub>2</sub>-10wt%FeO-MgO-MnO-P<sub>2</sub>O<sub>5</sub> slag (*R* = 2), whereas the content increases to 9.15 wt% on adding 11 wt% Al<sub>2</sub>O<sub>3</sub>. Wang [4] has also reported that the P<sub>2</sub>O<sub>5</sub> content in the P-rich phase reaches 28.71 wt% with the addition of 15.17 wt% Al<sub>2</sub>O<sub>3</sub> in CaO-SiO<sub>2</sub>-Fe<sub>1</sub>O-MgO-P<sub>2</sub>O<sub>5</sub> slag.

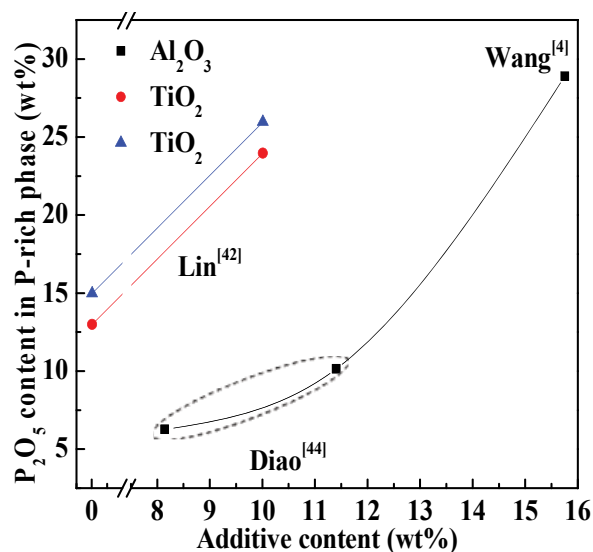
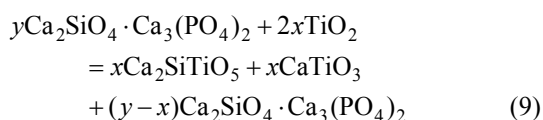
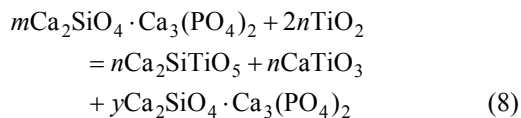


Fig. 15. Effect of addition of Al<sub>2</sub>O<sub>3</sub> and TiO<sub>2</sub> on selective enrichment of phosphorus

Similarly, the mechanism of TiO<sub>2</sub> modification is shown in Eqs. (8-9) [45]. CaSiTiO<sub>5</sub> and CaTiO<sub>3</sub> are generated on adding TiO<sub>2</sub>. Lin [45] has found that the P<sub>2</sub>O<sub>5</sub> content in the P-rich phase is only 13-15 wt% and increases to 24-26 wt% on adding 10 wt% TiO<sub>2</sub>.



The effect of Al<sub>2</sub>O<sub>3</sub> and TiO<sub>2</sub> on the selective enrichment of the P-rich phase is significant. The P<sub>2</sub>O<sub>5</sub> content in the P-rich phase reaches 20 wt% on adding 15 wt% Al<sub>2</sub>O<sub>3</sub> or 10 wt% TiO<sub>2</sub> to the slag.

#### 4. Selective growth and precipitation in dephosphorization slag

##### 4.1. Effect of temperature on selective growth and precipitation

According to the mechanism of selective enrichment and separation by Sui, the enrichment phase will grow up by control-

ling temperature, slag basicity, slag composition, and additives. Finally, the efficiency of separating valuable components is improved. The process is called as selective growth.

Heat treatment is the main factor affecting selective growth and precipitation. Most reports agree that the P-rich phase is thicker at lower cooling rates [4,5,7,23,47].

Wang [4] has analyzed the crystallization of the P-rich phase in CaO-SiO<sub>2</sub>-Fe<sub>t</sub>O-MgO-P<sub>2</sub>O<sub>5</sub>-Al<sub>2</sub>O<sub>3</sub>/TiO<sub>2</sub> slag by differential scanning calorimetry. The results reveal that the crystallization temperature of the P-rich phase increases with decreasing cooling rate. The diffusion of the P-rich phase is hampered at higher sub-cooling degrees. Li [7] has reported the effect of temperature on selective growth in CaO-FeO-Fe<sub>2</sub>O<sub>3</sub>-SiO<sub>2</sub>-P<sub>2</sub>O<sub>5</sub> slag. The results reveal that the size of the P-rich phase and its crystal fraction are 40 μm and 24% at a cooling rate of 3°C/min, respectively, and the latter reaches its maximum value within 1 h. Wu [23] has examined the average size of P-rich phases in industrial SiO<sub>2</sub>-modified slag. On decreasing the cooling rate from 5°C·min<sup>-1</sup> to 3°C·min<sup>-1</sup> and 1°C·min<sup>-1</sup>, the average size increases from 8 μm to 56 μm and 87 μm and the P<sub>2</sub>O<sub>5</sub> content in the P-rich phase increases from 3.65 wt% to 7.5 wt% and 7.74 wt%, respectively. Yang [47] has analyzed the growth of the P-rich phase in CaO-SiO<sub>2</sub>-Fe<sub>2</sub>O<sub>3</sub>-MgO-MnO-P<sub>2</sub>O<sub>5</sub>-Al<sub>2</sub>O<sub>3</sub>-TiO<sub>2</sub> slag at 1520°C. The statistical results show that the relationship between holding time (*t*) and the size of the C<sub>2</sub>S layer (*D*) can be described by  $D = kt^m$ . Where, *k* and *m* is constant. Thus, the size of the P-rich phase exceeds 40 μm when the cooling rate is less than 3°C·min<sup>-1</sup>.

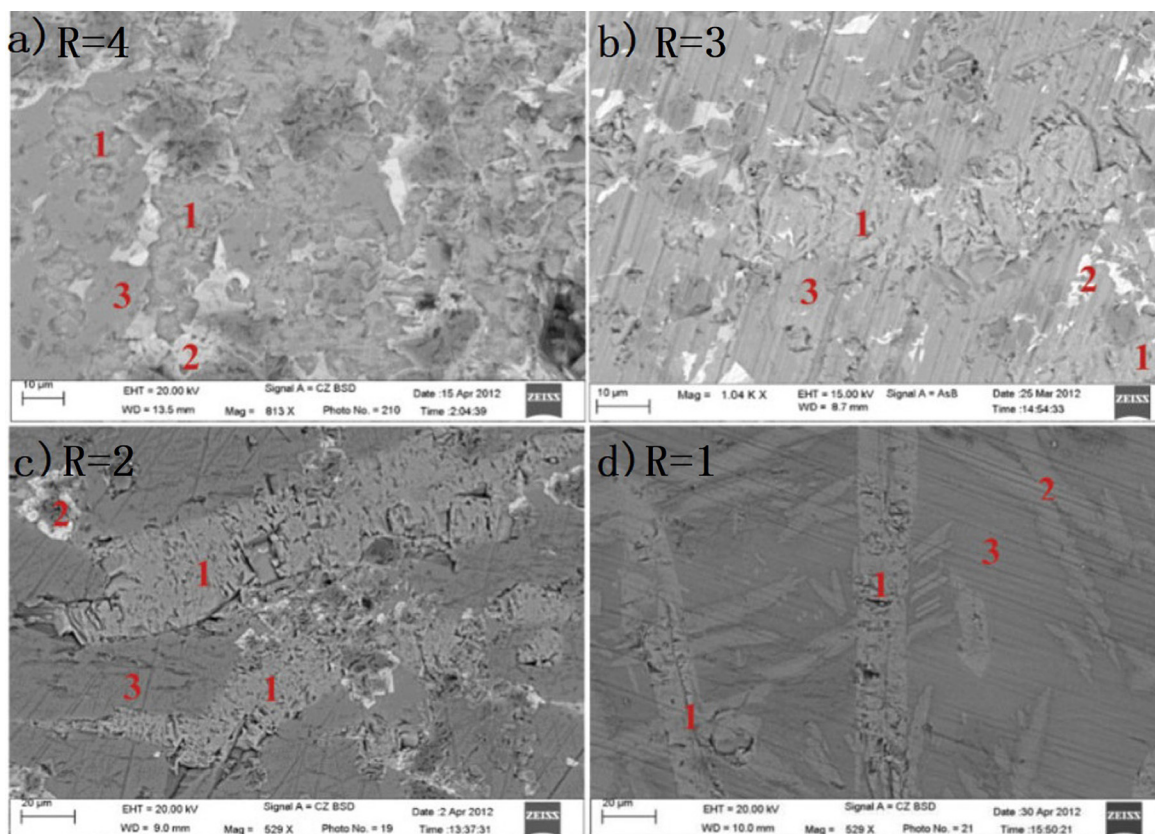


Fig. 16. Size of different phases (1: P-rich phase, 2: RO phase, 3: matrix phase) [8]

#### 4.2. Effect of slag basicity and composition on selective growth and precipitation

Appropriate slag basicity and composition promote the selective growth and precipitation of the P-rich phase [8,9,15]. As shown in Fig. 16, the size of the P-rich phase is 10-30  $\mu\text{m}$ , 20-100  $\mu\text{m}$ , and 30-150  $\mu\text{m}$  at  $R = 4, 3,$  and  $2,$  respectively [8]. Further, the P-rich phase at  $R = 1$  is rod-shaped and smaller than that at  $R = 2$ .

As MgO and MnO enter the RO phase, they have little effect on the selective growth and precipitation of the P-rich phase. Moreover, few studies have focused on the influence of  $\text{P}_2\text{O}_5$  and  $\text{Fe}_t\text{O}$  contents on the selective growth and precipitation of phosphorus [9,15]. Zhou [9] has measured the size of the P-rich phase in  $\text{CaO-Fe}_t\text{O-SiO}_2\text{-P}_2\text{O}_5$  slag. On increasing the  $\text{P}_2\text{O}_5$  content from 6 wt% to 10 wt% and 18 wt%, the size of the P-rich phase increases from 20-60  $\mu\text{m}$  to 30-90  $\mu\text{m}$  and 50-80  $\mu\text{m}$ , respectively.

#### 4.3. Effect of additives on selective growth and precipitation

Recently, some studies focusing on the effect of additives ( $\text{CaF}_2$ ,  $\text{Na}_2\text{O}$ ,  $\text{Al}_2\text{O}_3$ , and  $\text{TiO}_2$ ) on the selective growth and precipitation of the P-rich phase have found  $\text{CaF}_2$  and  $\text{Al}_2\text{O}_3$

have a positive effect [40,42]. According to Fig. 17a-b, the size of the P-rich phase is 20-40  $\mu\text{m}$  on the addition of 3 wt%  $\text{CaF}_2$  and increases to 100  $\mu\text{m}$  on adding 6 wt%  $\text{CaF}_2$  [40].

Jiang [42] has reported the effect of  $\text{Al}_2\text{O}_3$  on the selective growth of the P-rich phase in  $\text{CaO-SiO}_2\text{-Fe}_2\text{O}_3\text{-MgO-MnO-P}_2\text{O}_5\text{-Al}_2\text{O}_3$  slag. As shown in Fig. 18, the P-rich phase is significantly accumulated on the addition of  $\text{Al}_2\text{O}_3$ , and the size of the P-rich phase increases from 20  $\mu\text{m}$  (without  $\text{Al}_2\text{O}_3$ ) to 30-40  $\mu\text{m}$  on the addition of 8 wt%  $\text{Al}_2\text{O}_3$ .

### 5. Separation of phosphorus from dephosphorization slag

#### 5.1. Magnetic separation of dephosphorization slag

##### 5.1.1. Effect of Slag Basicity and Composition on Magnetic Separation

A common method for separating dephosphorization slag is magnetic separation. The phosphorus recovery rate can be promoted under a suitable magnetic field intensity ( $<0.5$  T) and slag size ( $<50$   $\mu\text{m}$ ) [5,7,8,12,25,40,41,54-58]. Several parameters have been suggested to characterize magnetic separation [12].

$$L_p = \frac{\omega_{(\text{P}_2\text{O}_5)_1} \cdot M_1}{\omega_{(\text{P}_2\text{O}_5)_2} \cdot M_2} \quad (10)$$

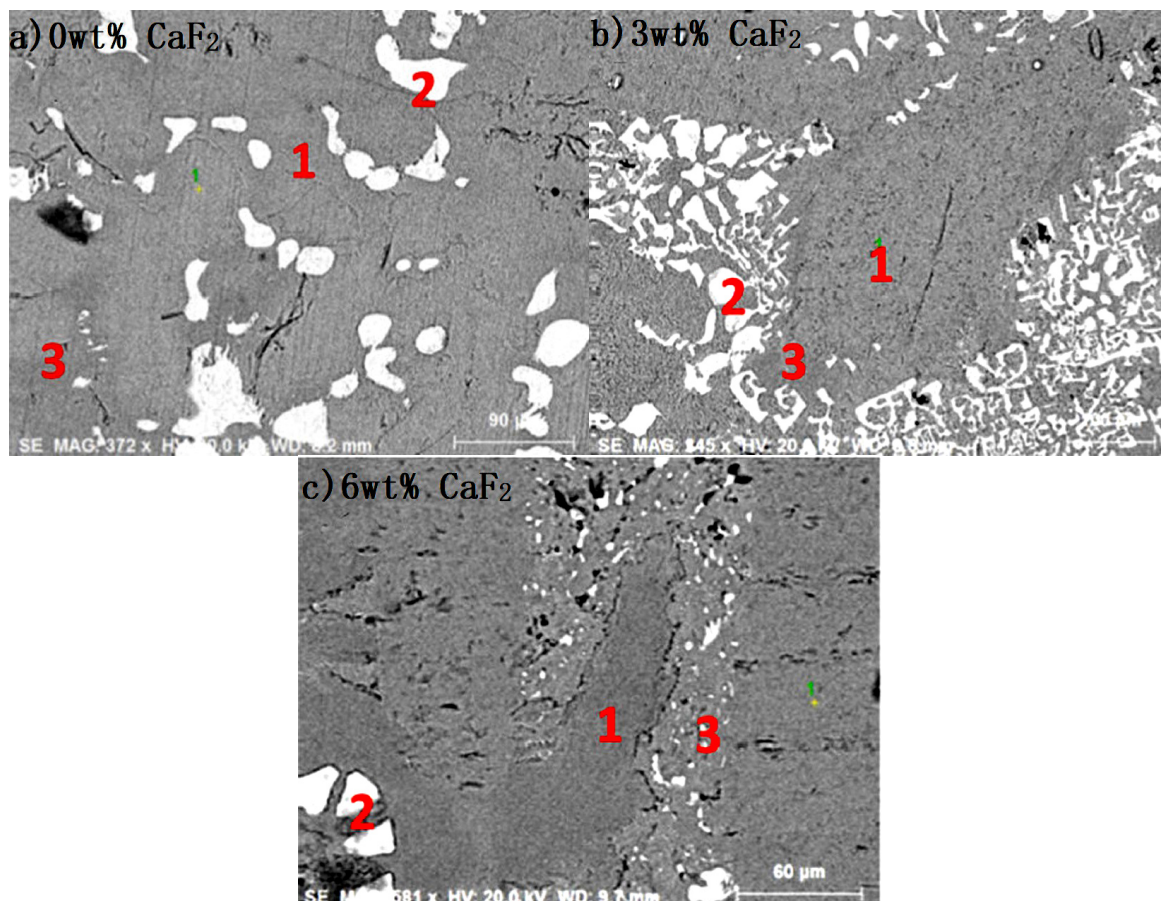


Fig. 17. Effect of  $\text{CaF}_2$  on selective growth (1: P-rich phase, 2: RO phase, 3: matrix phase) [40]

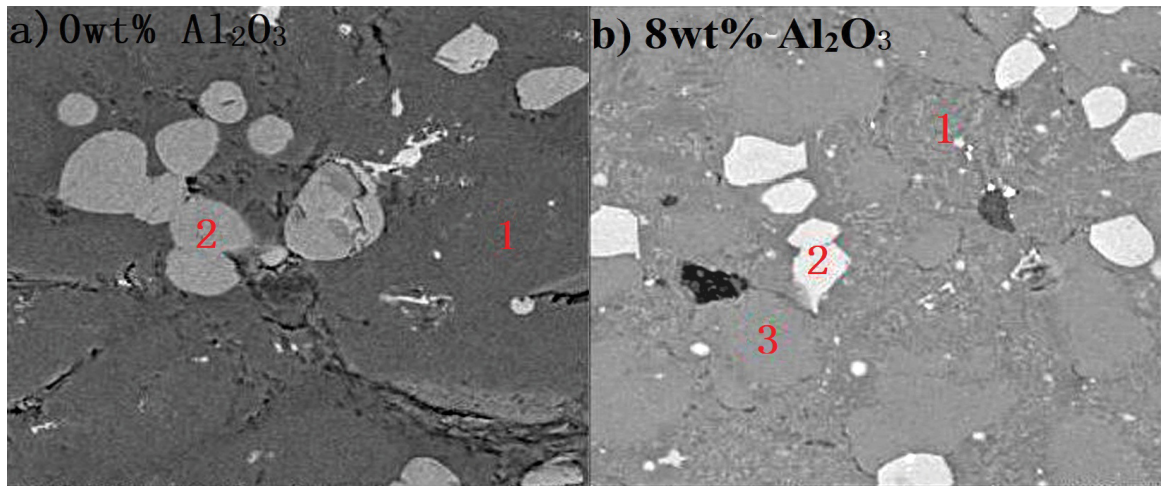


Fig. 18. Effect of  $\text{Al}_2\text{O}_3$  on selective growth (1: P-rich phase, 2: RO phase, 3: matrix phase) [42]

$$H_{P,i} = \frac{\omega_{(\text{P}_2\text{O}_5)_1} \cdot M_1}{\omega_{(\text{P}_2\text{O}_5)_1} \cdot M_1 + \omega_{(\text{P}_2\text{O}_5)_2} \cdot M_2} \quad (i = 1 \text{ or } 2) \quad (11)$$

$$H_{\text{Fe},i} = \frac{\omega_{(\text{TFe})_1} \cdot M_1}{\omega_{(\text{TFe})_1} \cdot M_1 + \omega_{(\text{TFe})_2} \cdot M_1} \quad (i = 1 \text{ or } 2) \quad (12)$$

Where  $M_1$  and  $M_2$  are the mass of the nonmagnetic and magnetic substances (g), respectively;  $\omega_{(\text{P}_2\text{O}_5)_1}$  and  $\omega_{(\text{P}_2\text{O}_5)_2}$  are the mass fractions of  $\text{P}_2\text{O}_5$  in the nonmagnetic and magnetic substances (%), respectively;  $L_p$  is the phosphorus partition ratio between the nonmagnetic and magnetic substances;  $\omega_{(\text{TFe})_1}$  and  $\omega_{(\text{TFe})_2}$  are the mass fractions of the nonmagnetic and magnetic substances (%), respectively;  $H_p$  is the  $\text{P}_2\text{O}_5$  content (wt %) in the slag entering the nonmagnetic and magnetic substances; and  $H_{\text{Fe}}$  is the TFe content (wt %) in the slag entering the nonmagnetic and magnetic substances. The phosphorus recovery rate and iron recovery rate are defined by the  $\text{P}_2\text{O}_5$  content entering the nonmagnetic substances and Fe content entering the magnetic substances, respectively.

Suitable slag basicity and compositions promote magnetic separation. Lin [12,15] has examined the effect of slag basicity on magnetic separation in  $\text{CaO-SiO}_2\text{-Fe}_2\text{O}_3\text{-MgO-P}_2\text{O}_5\text{-MnO-Al}_2\text{O}_3/\text{TiO}_2/\text{CaF}_2$  slag. When the  $R$  is decreased from 4 to 2, the  $\text{P}_2\text{O}_5$  content in the slag entering the nonmagnetic substance increases from 64.59 wt% to 74.68 wt% and the  $L_p$  changes from 2.71 to 5.48. Moreover, as shown in Fig. 19, the phosphorus recovery rate increases from 73.5% to 84.57% when the  $R$  decreases from 4 to 2. Diao [58] has reported magnetic separation in  $\text{CaO-10wt}\%\text{SiO}_2\text{-Fe}_2\text{O}_3\text{-MgO-MnO-10wt}\%\text{P}_2\text{O}_5\text{-Al}_2\text{O}_3/\text{TiO}_2$  slag ( $R = 2.5$ ). According to Figure 18, the phosphorus recovery rate in the nonmagnetic substances is 74%.

$\text{MgO}$  and  $\text{MnO}$  improve slag metallization and the magnetism of the iron-rich phase, resulting in the incomplete separation of phosphorus and iron [15,58]. As shown in Figure 18, on adding 10 wt%  $\text{MgO}$  and 10 wt%  $\text{MnO}$  to the slag, the phosphorus recovery rate in the nonmagnetic substances decreases from 65.44% to 40.43% and 35.8%. and  $L_p$  decreases from 2.71 to

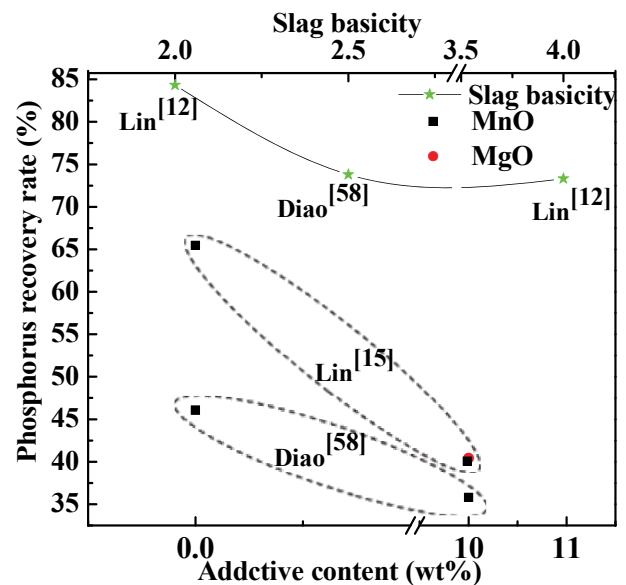


Fig. 19. Effect of slag basicity and compositions on magnetic separation

0.63 and 0.56, respectively [15.] Diao [58] has added 10 wt%  $\text{MnO}$  into  $\text{CaO-SiO}_2\text{-Fe}_2\text{O}_3\text{-MgO-MnO-10wt}\%\text{P}_2\text{O}_5$  slag and has found that the phosphorus recovery rate decreases from 46% to 40%. Thus, the phosphorus recovery rate can exceed 70% when the slag basicity is 1.5-2.5. Further,  $\text{MgO}$  and  $\text{MnO}$  decrease the phosphorus recovery rate.

### 5.1.2. Effect of Additives on Magnetic Separation

Many studies [40-41,58] have revealed that  $\text{CaF}_2$  and  $\text{Na}_2\text{O}$  improve slag metallization and the magnetism of the iron-rich phase. Moreover, they can result in the incomplete separation of phosphorus and iron. However,  $\text{Al}_2\text{O}_3$  and  $\text{TiO}_2$  are beneficial to magnetic separation.

Lin [40-41] has analyzed the phosphorus recovery rate in fluorine-free modified slag. As shown in Fig. 20, the phosphorus recovery rate is 64.6% in fluorine-free modified slag, while

it decreases to 48.8% on adding 6 wt%  $\text{CaF}_2$ . In addition, the phosphorus recovery rate is 64.55% on adding less than 6 wt%  $\text{Na}_2\text{O}$ , but it is only 36.53% on adding more than 6 wt%  $\text{Na}_2\text{O}$ . Therefore, the  $\text{Na}_2\text{O}$  content should be controlled to be within 6 wt%.

According to Fig. 21, the phosphorus recovery rate is 45.51 wt% in  $\text{Al}_2\text{O}_3$ -free slag and increases to 68.47 wt% and 82.16 wt% on increasing the  $\text{Al}_2\text{O}_3$  content from 10 wt% to 15 wt%. Furthermore, the phosphorus recovery rate increases to 74.46 wt% on adding 10 wt%  $\text{TiO}_2$ . Additionally, the  $L_p$  is 4.61 and 2.91 on adding 10 wt%  $\text{Al}_2\text{O}_3$  and 10 wt%  $\text{TiO}_2$ , respectively [12]. Simultaneously, Diao [58] has reported the effect of  $\text{Al}_2\text{O}_3$  and  $\text{TiO}_2$  on magnetic separation in  $\text{CaO-SiO}_2\text{-Fe}_t\text{O-MgO-MnO-10 wt% P}_2\text{O}_5$  slag. The results reveal that the phosphorus recovery rate reached 87% and 70% on the addition of 10 wt%  $\text{Al}_2\text{O}_3$  and 10 wt%  $\text{TiO}_2$ , respectively.

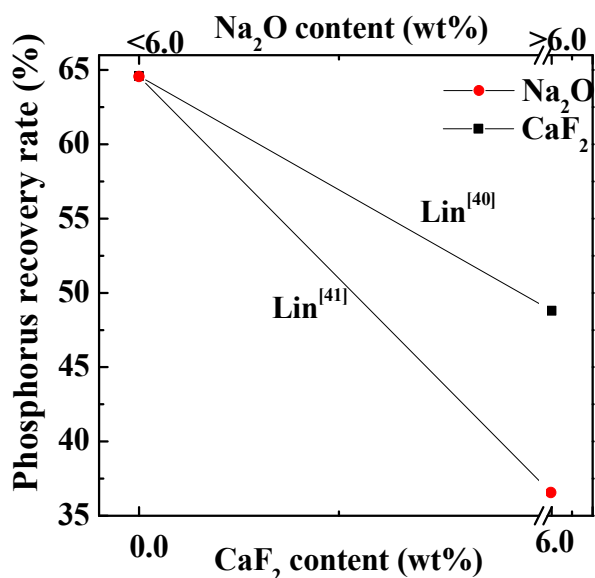


Fig. 20. Effect of  $\text{CaF}_2$  and  $\text{Na}_2\text{O}$  contents on magnetic separation

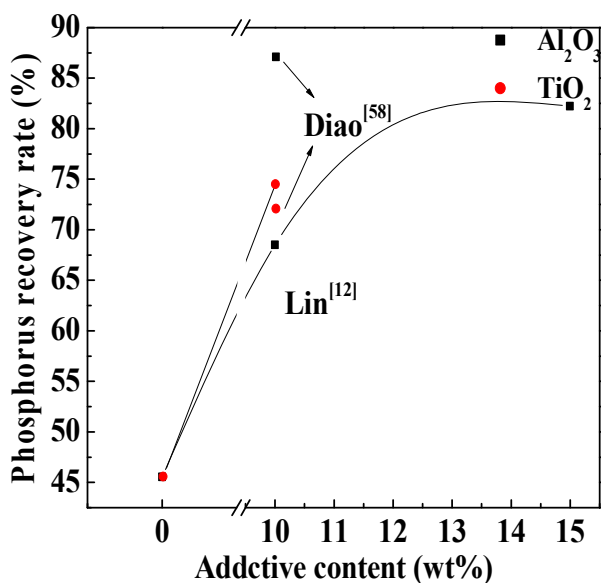


Fig. 21. Effect of  $\text{Al}_2\text{O}_3$  and  $\text{TiO}_2$  contents on magnetic separation

In summary, the phosphorus recovery rate increases to 60% either in fluorine-free modified slag or in slag containing 6 wt%  $\text{Na}_2\text{O}$ . Moreover, it reaches 70% on adding more than 10 wt%  $\text{Al}_2\text{O}_3$  and 10 wt%  $\text{TiO}_2$ .

## 5.2. Separation of phosphorus from dephosphorization slag by supergravity separation

Previous studies have reported that calcium silicate in slag floats to the top due to the density difference between calcium silicate and the slag. Namely,  $\text{CaO}$ ,  $\text{SiO}_2$ , and  $\text{P}_2\text{O}_5$  accumulate at the top of the slag. Meanwhile,  $\text{FeO}$ ,  $\text{Fe}_2\text{O}_3$ , and  $\text{MnO}$  accumulate at the bottom of the slag [48,49]. However, the initial temperature must be up to  $1580^\circ\text{C}$  and the average cooling rate should be less than  $2^\circ\text{C}\cdot\text{min}^{-1}$ . Additionally,  $\text{FeO}$  and  $\text{MnO}$  contents must be more than 30% [48]. Supergravity separation has been found to be effective for phosphorus separation [50-53].

Li [50-52] has reported the separation of Fe-bearing and P-bearing phases in industrial slag. As shown in Fig. 22, the sample obtained by centrifugal enrichment ( $G = 800$ ,  $T = 1663\text{ K}$ ,  $t = 40\text{ min}$ ) is compared with a parallel sample ( $G = 1$ ,  $T = 1663\text{ K}$ ,  $t = 40\text{ min}$ ). According to Fig. 22a, a uniform structure is observed under normal gravity. However, an obvious stratified boundary appears after centrifugal enrichment (as depicted in the white line in Figure 21b). The bottom of the sample is compact and tight, while the top, where the P-rich phase is formed, is loose and porous [50]. Therefore, the enrichment efficiency is proportional to the centrifugation time and gravity coefficient.

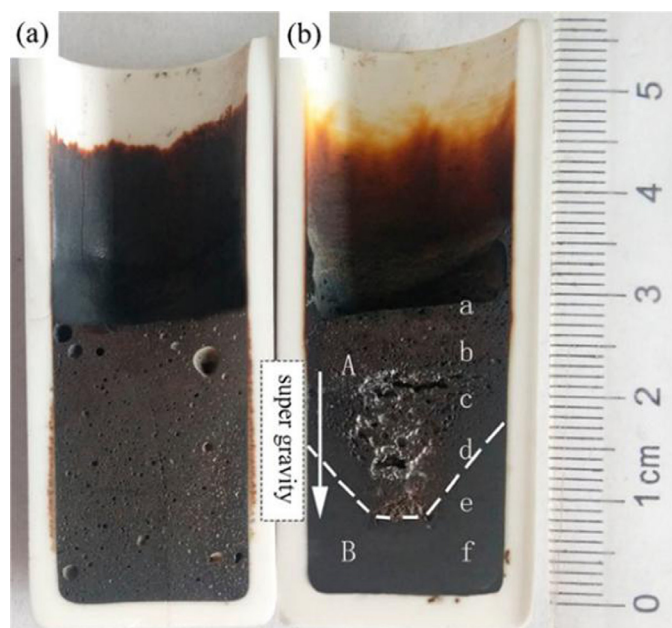


Fig. 22. Cross-section of the sample (a: parallel sample, b: sample after centrifugal enrichment) [50]

Li [50] has reported the separation of the Fe-bearing phase and P-rich phase in industrial slag ( $G = 800$ ,  $T = 1663\text{ K}$  and

$t = 40$  min). The slag is fully mixed and 2 wt%  $\text{CaF}_2$  is added. As shown in Fig. 23, the maximum mass fractions of  $\text{P}_2\text{O}_5$  and  $\text{Fe}_t\text{O}$  in the P-rich and Fe-bearing phases are 4.12 wt% and 35.17 wt% and their recovery ratios are 77.56% and 60.18%, respectively. However, when  $G = 600$ ,  $T = 1663$  K, and  $t = 15$  min, the mass fraction of  $\text{P}_2\text{O}_5$  in the P-rich phase is 3.56 wt% and that of  $\text{Fe}_t\text{O}$  in the Fe-bearing phase is 38.67 wt% and the recovery ratios of  $\text{P}_2\text{O}_5$  and  $\text{Fe}_t\text{O}$  are 82.2% and 68.5%, respectively [51]. Additionally, Li [52] has revealed the separation of  $\text{P}_2\text{O}_5$  and  $\text{Fe}_t\text{O}$  in  $\text{CaO-SiO}_2\text{-FeO-MgO-P}_2\text{O}_5$  slag ( $G = 700$ ,  $T = 1623$  K, and  $t = 20$  min). The recovery ratios of  $\text{P}_2\text{O}_5$  and  $\text{Fe}_t\text{O}$  are 76.67% and 85.02%, respectively. Gao [53] has also analyzed the separation of the Fe-bearing and P-bearing phases in high-phosphorous oolitic iron ore at  $1200^\circ\text{C}$  and  $G = 1200$ . The recovery ratios of  $\text{P}_2\text{O}_5$  and  $\text{Fe}_t\text{O}$  are 99.19% and 95.83%, respectively.

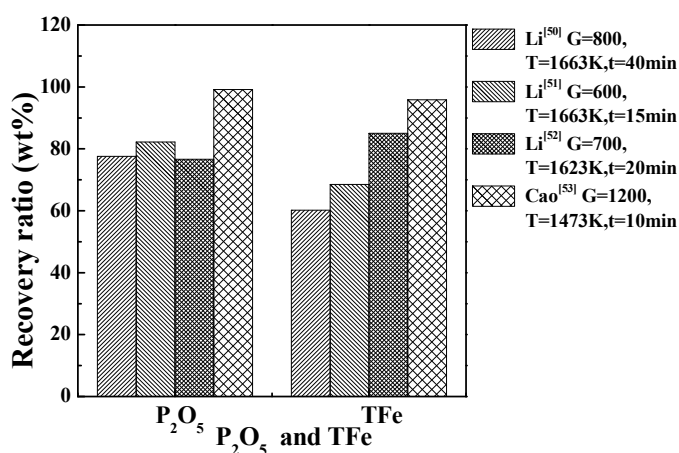


Fig. 23. Recovery ratio of  $\text{P}_2\text{O}_5$  and  $\text{Fe}_t\text{O}$

Consequently, the enrichment efficiency can be promoted by supergravity. Thus, the supergravity method is effective for the separation of the Fe-bearing and P-rich phases.

## 6. Summary and future applications

All the above studies have investigated the formation and evolution of phases in dephosphorization slag. Further, instructive data concerning the effect of various factors (slag basicity, slag composition, and additives) on the selective enrichment, growth, and separation of phosphorus have been obtained. However, most these studies have focused on laboratory investigations; therefore, the application in industrial production is still unclear.

Recently, the dephosphorization in hot metal pretreatment and previous stage of the steelmaking still utilize  $\text{CaO-FeO-SiO}_2$  slag. The removal of phosphorus is thermodynamically favorable before decarburization because of the relatively low temperature. However, an increase in the dephosphorization efficiency is greatly limited due to the higher melting point and poor liquidity. Actually,  $\text{Al}_2\text{O}_3$ ,  $\text{Na}_2\text{O}$ , and  $\text{TiO}_2$  decrease the melting point and improve the liquidity. On the other hand, they

replace parts of  $\text{SiO}_2$  and combine with  $\text{CaO}$  to generate new phases (decreasing the value of “ $n$ ” in  $n\text{C}_2\text{S-C}_3\text{P}$ ). Therefore, the process not only effectively increases the  $\text{P}_2\text{O}_5$  content in the P-rich phase but also promotes the magnetic separation of this phase. Further,  $\text{Na}_2\text{O}$  strengthens the magnetism of the Fe-bearing phase and has little effect on the magnetic separation. Li [61] has revealed that according to thermodynamics,  $\text{Al}_2\text{O}_3/\text{TiO}_2$  slightly decreases the distribution ratio between the slag and carbon-saturated iron. However, according to semi-industrial test results,  $\text{Al}_2\text{O}_3/\text{TiO}_2$  significantly improves the dephosphorization efficiency of the previous stage in the steelmaking process (before decarburization;  $[\text{C}] = 2.5\text{-}3.0\%$ ). The results show that the dephosphorization efficiency is up to 85% and the  $[\text{P}]$  content is less than 0.02% [62,63], which is beneficial to the smelting of medium and high-phosphorus-content hot metals. Additionally, it broadens the range of available iron ore resources and increases the purity of steel.

Therefore,  $\text{CaO-FeO-SiO}_2\text{-Al}_2\text{O}_3/\text{TiO}_2/\text{Na}_2\text{O}$  dephosphorization slag is significant for improving production efficiency and resource utilization. Previous studies have analyzed the behaviors of phosphorus enrichment and separation under the conditions of thermodynamics/dynamics. To effectively increase the practical application of dephosphorization slag, further research concerning phosphate fertilizers are necessary. Although  $\text{Al}_2\text{O}_3/\text{TiO}_2/\text{Na}_2\text{O}$  enriches the P-rich phase, how the proportion of the P-rich phase in dephosphorization slag changes with different compositions directly affects the total  $\text{P}_2\text{O}_5$  solubility in the slag. Moreover, few investigations have focused on the most direct data related to the quantity of dephosphorization slag. The  $\text{P}_2\text{O}_5$  content in the slag increases with increasing dephosphorization efficiency. However, the variation in slag viscosity and slag structure caused by  $\text{P}_2\text{O}_5$  content affects the liquidity and separation of the slag. Therefore, further studies on these aspects should be conducted.

## Acknowledgement

The authors would like to thank the National Natural Science Foundation of China (No. 51474021) for financial support.

## REFERENCES

- [1] S. Jung, Y. Do, J. Choi, *Steel Res. Int.* **77** (2006).
- [2] H. Ono, A. Inagaki, T. Masui, N. Hiroshi, N. Shoji, *ISIJ Int.* **21** (2), 135-144 (1980).
- [3] H.J. Li, *ISIJ Int.* **35** (9), 1079-1088(1995).
- [4] Z.J. Wang. Investigation on Physical and Chemical Properties of P-bearing Steelmaking Slags during the Selective Enrichment Process of Phosphorus. PhD thesis, University of Science & Technology Beijing, June.
- [5] Z.T. Sui, B.C. Chen, in: *Proceedings of the National Powder Engineering Conference, China 1998*.
- [6] Z.T. Sui, T.P. Lou, N.X. Fu, CN1253185, China 2000.

- [7] J.Y.Li. Selective enrichment and phase separation of phosphate in steelmaking slags. PhD thesis, University of Science & Technology Beijing, December.
- [8] L. Lin, Y.P. Bao, M. Wang, *Ironmaking and Steelmaking* **40** (7), 521-527 (2013).
- [9] H.M. Zhou, Y.P. Bao, L. Lin, *China Metall.* **23** (1), 45-49 (2013).
- [10] S. Ken-Ichi, K. Shin-Ya, H. Shibata, *Tetsu-to-Hagane* **49** (49), 505-511(2009).
- [11] H.M. Zhou, Y.P. Bao, L. Lin, *Steel Res. Int.* **84** (9), 863-869 (2013).
- [12] L. Lin, Y.P. Bao, M. Wang, *Ironmaking and Steelmaking* **21** (5), 496-502 (2014).
- [13] L.C. He, Y.M. Wang, *Fertilizer industry knowledge, 1975*, Fuel Chemical Industry Press, Beijing(in Chinese).
- [14] H.G. Jin, L.B. Yu, *China Res. Comp. Util.* **3**, (1999).
- [15] L. Lin, Y.P. Bao, M. Wang, *High Temp. Mater. Proc.* **35** (4), 425-432 (2016).
- [16] L. Lin, Y.P. Bao, M. Wang, *ISIJ Int.* **54** (12), 2746-2753 (2014).
- [17] J. Diao, L. Jiang, Y. Wang, *Phosphorus Sulfur* **190** (3), 387-395 (2014).
- [18] L.S. Li, X.F. Yu, X.R. Wu, *P. Soc. Photo-Opt. Ins.* **10** (1), 78-81 (2006).
- [19] L.S. Li, X.F. Yu, *China Metal.* **17** (1), 42-45 (2007).
- [20] S. Fukagai, T. Hamano, F. Tsukihashi, *ISIJ Int.* **47** (1), 187-189 (2007).
- [21] X. Yang, H. Matsuura, F. Tsukihashi, *Metal. Mater. Trans. B* **51** (9), 1298-1307 (2010).
- [22] H.J. Guo, *Metallurgical Physical Chemistry Tutorial, 2006*, Metallurgical Industry Press, Beijing(in Chinese).
- [23] X.G. Wu, J.N. An, *J. Anhui Univ. Technology* **27** (3), 233-237(2010).
- [24] H. Ono, *Tetsu-to-Hagane* **3**, (1980).
- [25] K. Ito, M. Yanagisawa, N. Sano, *Tetsu-to-Hagane* **68** (2), 342-344 (1982).
- [26] N. Wang, Z.G. Liang, M. Chen, *Northeast Univ. J.* **32** (6), 814-817 (2011).
- [27] X.F. Dou, M.M. Zhu, T.C. Lin, *Chongqing Univ. J.* **38** (5), 78-82 (2015).
- [28] X. Yang, H. Matsuura, F. Tsukihashi, *ISIJ Int.* **49** (9), 1298-1307 (2009).
- [29] X. Yang, H. Matsuura, F. Tsukihashi, *ISIJ Int.* **50** (5), 702-711 (2010).
- [30] X. Yang, H. Matsuura, F. Tsukihashi, *Tetsu-to-Hagane* **95** (95), 268-274 (2009).
- [31] H. Suito, R. Inoue, *T. Iron Steel I. Jpn.* **46** (2), 180-187 (2006).
- [32] R. Inoue, H. Suito, *ISIJ Int.* **46** (2), 174-179 (2006).
- [33] C. Su, L.Z. Chang, in: *Proceedings of the National Metallurgical Energy Environmental Protection Production Technology Association, China 2014*.
- [34] M.C. Jha, G.R. Wicker, US4110400, US 1978.
- [35] P. Zhang, Z. Sui, *Metall. Metal. Mater. Trans. B* **26** (2), 345-351 (1995).
- [36] P.K. Son, Y. Kashiwaya, *Tetsu-to-Hagane* **48** (9), 1165-1174 (2008).
- [37] X.M. Yang, J.P. Duan, C.B. Shi, *Metal. Mater. Trans. B* **42** (4), 738-770 (2011).
- [38] X.M. Yang, C.B. Shi, Z. Meng, *Metal. Mater. Trans. B* **42** (1), 951-977 (2011).
- [39] Y.Liu, Q.F. Shu, *Nonferrous Metal. Sci. Eng.* **7** (3), 29-34 (2016).
- [40] L. Lin, Y.P. Bao, Q. Yang, *Ironmaking and Steelmaking* **42** (3), 331-338 (2015).
- [41] L. Lin, Y.P. Bao, W. Jiang, *ISIJ Int.* **55** (3), 552-558 (2015).
- [42] L. Jiang, J. Diao, X.M. Yan, *Proceedings of the National Powder Engineering Conference, China 2014*.
- [43] X.L. Pan, J.Y. Li, M. Guo, *J. Iron Steel Res.* **29** (6), 474-480 (2017).
- [44] L. Jiang, J. Diao, X.M. Yan, *ISIJ Int.* **55** (3), 564-569 (2015).
- [45] L. Lin, Y.P. Bao, M. Wang, *Chinese J. Eng.* **8** (1), 1013-1019 (2014).
- [46] Z.M. Wang. *The Study on the Separation and Growing up of Perovskite Phase from the Blast Furnace Slag Containing Titanium*. PhD thesis, Northeastern University, June.
- [47] G.M. Yang, X.R. Wu, L.S. Li, *Can. Metall. Quart.* **51** (2), 150-156 (2012).
- [48] H. Ono, A. Inagaki, T. Masui, *ISIJ Int.* **21** (2), 135-144 (1980).
- [49] H. Ono, A. Inagaki, T. Masui, H. Narita, *Tetsu-to-Hagane* **66** (9), 1317-1326 (1980).
- [50] C. Li, J.T. Gao, F.Q. Wang, *Ironmaking and Steelmaking*, 1-6 (2016).
- [51] C. Li, J. Gao, Z. Wang, *ISIJ Int.* **57** (4), 4 (2017).
- [52] C. Li, J. Gao, Z.C. Guo, *Metal. Mater. Trans. B* **47** (3), 1516-1519 (2016).
- [53] J. Gao, Y. Zhong, L. Guo, *Metal. Mater. Trans. B* **47** (2), 1080-1092 (2016).
- [54] K. Yokoyama, H. Kubo, K. Mori, *T. Iron Steel I. Jpn.* **47** (10), 1541-1548 (2007).
- [55] H. Kubo, M.Y. Kazuyo, T. Nagasaka, *T. Iron Steel I. Jpn.* **50** (1), 59-64 (2009).
- [56] X.R. Wu, G.M. Yang, L.S. Li, *Ironmaking and Steelmaking* **41** (5), 335-341(2014).
- [57] M.Y. Kazuyo, *Trans. T. Iron Steel I. Jpn.* **50** (3), 306-312 (2010).
- [58] J. Diao, B. Xie, Y. Wang, *ISIJ Int.* **52** (6), 955-959 (2012).
- [59] Y.H. Wang, B. Xie, J. Diao, *Chinese J. Eng.* **33** (3), 323-327 (2011).
- [60] Z.H. Xu, *Steel slag phosphate fertilizer production, 1962*, China Industry Press, Beijing (in Chinese).
- [61] F.S. Li, X. Li, Y.L. Zhang, *Metal. Mater. Trans. B* **48** (5), 1-12 (2017).
- [62] F.S. Li, Y.L. Zhang, Z. Guo, *JOM-U.S.* **69** (2), 1624-1631 (2017).
- [63] F.S. Li, Y.L. Zhang, Z. Guo, *JOM-U.S.* **69** (9), 1632-1638 (2017).